IMAGE PROCESSING TECHNIQUES FOR CHARACTERISATION OF POLYMER WEAR DEBRIS

Pieter Samyn[1], Jan Quintelier[1], Patrick De Baets[1], Alessandro Ledda[2]

[1]*Ghent University – Laboratory Soete, Department Mechanical Construction and Production*
[2]Ghent University – TELIN
Sint-Pietersnieuwstraat 41 – 9000 Gent, Belgium
tel. +32 9 264 33 08 fax. +32 9 264 32 95

Contact person: Pieter.Samyn@UGent.be

Abstract

Wear debris particles were collected after sliding experiments on polyimide under different temperatures for quantification of their size and shape. Fourier spectra and morphological pattern spectra are analysed to extract parameters that relate to particle size and shape. The Fourier transform however lacks the ability to incorporate information about the particle shape, while Mathematical morphology (MM) allows for the determination of a structural element that is related to the debris morphology. Different spectral parameters are calculated and correlated to the physical occurrence of large agglomerated debris particles at high sliding temperatures. From the correlation coefficients between different spectrum parameters and their respective experimental parameters it is concluded that the mean and standard deviation of FFT spectra are proportional to temperature, while entropy is inversely proportional to normal load. Parameters calculated from a pattern spectrum generally provide better correlation with experimental sliding conditions compared to the FFT parameters, under conditions that the shape and threshold value of the filter element is appropriately chosen.

1. INTRODUCTION

Wear phenomena of polymers are either adhesive or abrasive and are characterised both by the formation of a polymer transfer film on the steel sliding surface and the formation of lost wear debris particles. In a strict sense, the polymer transfer film is not a wear product as it remains in the sliding interface and contributes to stable friction and wear processes by conglomeration and softening. The wear debris particles however are washed out towards the ends of the sliding stroke as separate particles and accumulate with progressive sliding. The sliding geometry has strong influence on the motion of the wear particles and the dynamics of wear debris compaction has been discussed by e.g. [1], determining for the transfer film thickness and amount of lost wear debris.

As such, the wear debris particles contains partial information about the wear mechanisms that has lead to disruption of the particle from the bulk and about a thermal cycle that it underwent under sliding [2]. The heat produced under sliding however may influence the polymer structure and transitions in mechanical properties contribute to softening or melting. A close examination on the polymer wear debris features is therefore interesting, revealing information about its shape and thermal characteristics. As an example for present investigation, the morphology of sintered polyimide wear debris is investigated after sliding under different temperatures between 60°C and 260°C under atmospheric conditions. Polyimides are used in situations requiring high-performance plastics where other engineering materials do not function, because of their unique combination of superior mechanical, chemical and thermal properties. Pioneering research on the tribological behaviour of polyimides and its self-lubricating ability in film or bulk material has been performed by Fusaro [3] and Tewari and Bijwe [4]. More recently, our research [5] shows severe transitions in friction and wear properties, which can be explained by an endothermal reaction in the polyimide bulktemperature and the reorientation of several functional groups relatively to the sliding surface. Present paper

investigates the properties of polyimide wear debris that was collected after sliding experiments under high temperature, after a presentation of the transitions in friction and wear.

2. FRICTION AND WEAR MEASUREMENTS

Sintered Vespel SP [6] polymer cylinders were reciprocating slid in counterformal contact against a high-alloy steel counterface under 50 N normal load and 0.3 m/s sliding velocity, as shown on the test rig in Figure 1. The temperature of the steel counterface is artificially controlled between 60°C and 260°C by resistance heating. A piezo-electrical force transducer is used to measure the friction force. The normal displacement of the cylinder towards its counterface is continuously measured by a contactless proximitor. The oscillating motion of the polymer sample is provided by a controlled variable-speed motor through an eccentric power transmission for adjustment of the stroke (15 mm). The normal load F_N is applied by a bridge, mechanically pulled down by a crank handle.

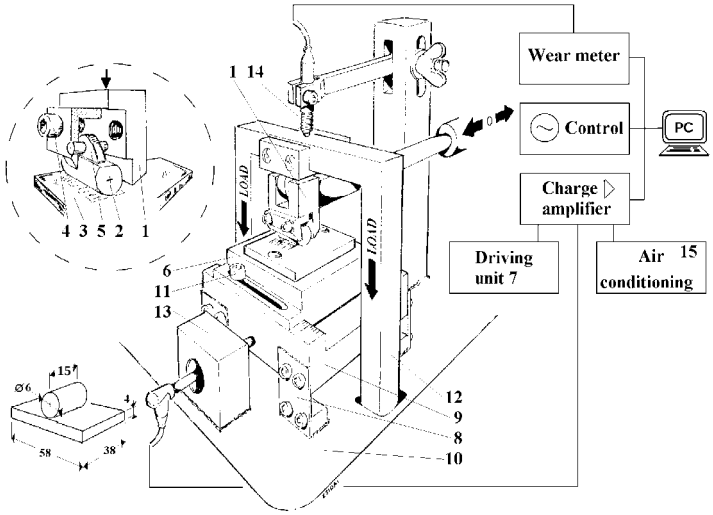

Figure 1. Friction and wear tester

The average friction coefficient after different sliding distances and final wear rates calculated from weight loss are represented in Figure 2, revealing a transition in both friction and wear at 180°C. At lower temperatures reasonably high friction occurs, while it suddenly drops above 180°C, corresponding to a stabilisation in wear rates.

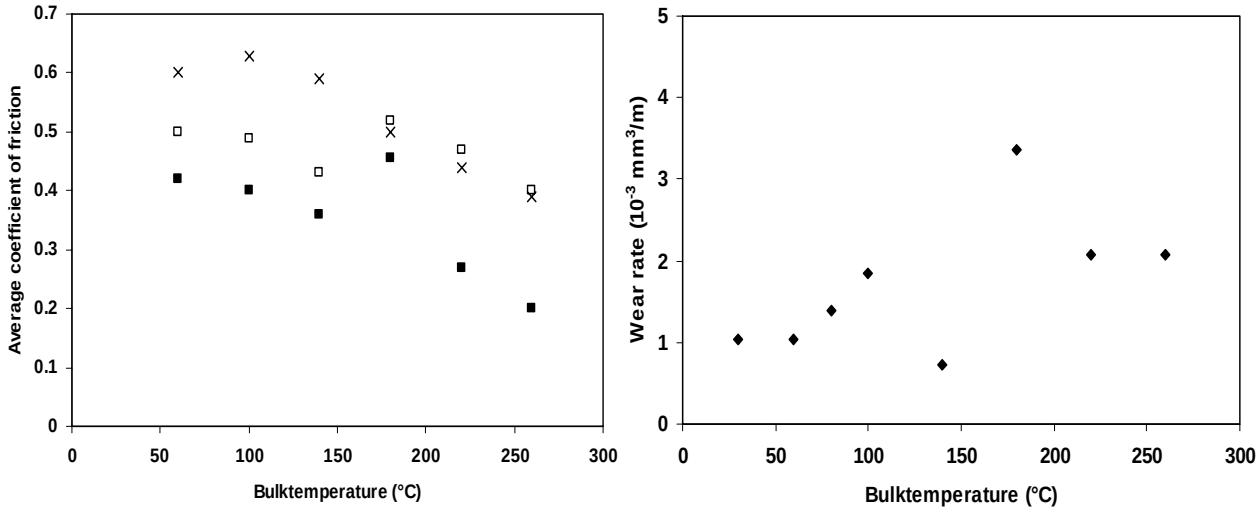

(a) (b)

Figure 2. (a) Friction coefficients after x 30 m, □ 100 m, ■ 15000 m and (b) wear rates after ♦ 15000 m as a function of applied bulktemperatures

3. WEAR DEBRIS CHARACTERISATION

3.1 Optical microscopy of wear debris

The wear debris produced after sliding experiments on sintered polyimide was collected and examined by optical microscopy as shown in Figure 3. It is clear that the wear debris morphology depends on the sliding temperature. Under 100°C there is only observed an amount of small wear debris particles, with rather scale-like shape. For sliding temperatures above 180°C, the particles become larger and consist of rather an agglomerated structure. Where large particles occur, wear rates increase or stabilise. The occurrence of large particles at 180°C is in accordance with the high wear rates measured in Figure 2, as it was reported by Fusaro [7] that the transferred particles might act as an abrasive third body. Due to their rather brittle nature, polyimides are however not resistant to abrasive wear. Slight plastification is only observed at 220°C and 260°C as some of the particles are glossy and become squeezed into the contact zone under shearing forces, with stabilisation in wear rates and formation of a transfer film. A detail of this type of agglomerated wear debris is shown in Figure 4 for the 260°C sliding test, reflecting a morphology that depends on the original sintered polyimide structure. According to catalogue information [6], the polyimide resins (powder) have an initial grain size diameter of 10 μm to 20 μm and are compacted towards 100 μm grains for beneficial flow characteristics into the sintering mould during a direct form sintering process. The pressure and temperature parameters of the subsequent sintering phases are however own to industrial proprietary. It seems that the agglomeration of separate grains correspond to the sintering process, with fracture of the grains under sliding occurring at weak sintered interfaces.

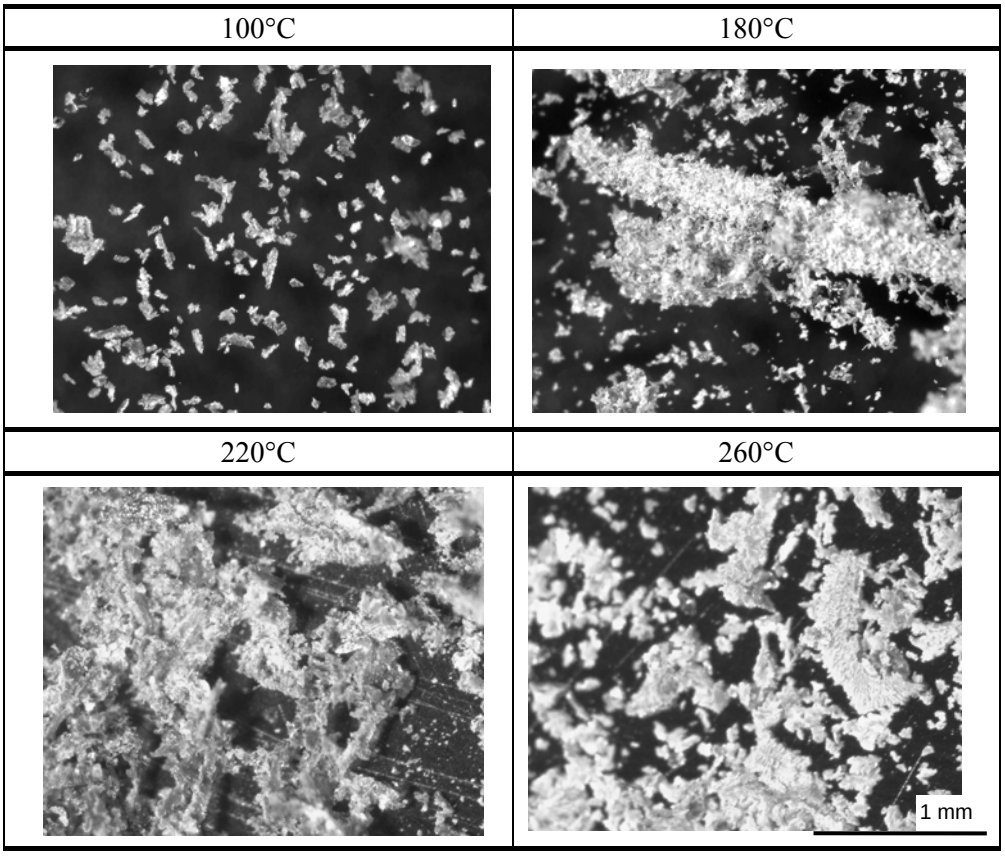

Figure 3. Changes in wear debris morphology depending on the sliding temperature

Other assumptions on the wear debris morphology were noted by e.g. Tewari and Bijwe [4], also observing a peak in both steady-state friction and wear with the position of the transition peaks depending on the sliding speed: while the friction peak occurred at 150°C, it seems however not

correlated to the wear peak that occurred at 200°C. They reported that the colour of wear debris varied with increasing temperature and become very dark at the temperature near the wear peak, indicating that thermal decomposition should be responsible for transitions and wear peaks.

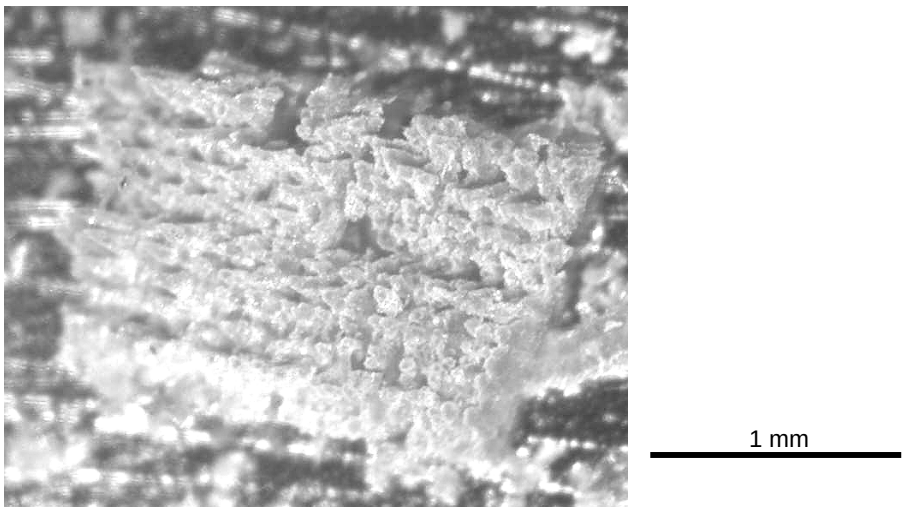

Figure 4. Detail of the wear debris morphology with agglomerated structure.

3.2 Thermal analysis of wear debris

The thermal stability and eventual thermal degradation of the polyimide wear debris was evaluated by performing differential thermal analysis (DTA) and thermogravimetric analysis (TGA). Figure 5a shows the TGA weight loss for original polyimide and wear debris after sliding under 100°C, 180°C and 260°C, while the DTA thermographs are represented in Figure 5b for the respective wear debris particles. Each sample is measured on approximately 3 mg of wear debris. It reveals that there is no thermal degradation of the polymer wear debris, which is for each sliding temperature restricted to 1 %. The initial increase in mass of about 1 % is due to small reactions on the wear debris, which have higher specific surface compared to the bulk polyimide sample. From the thermographs it seems that there is an endothermic reaction with maximum intensity at 180°C for each of the wear debris particles. However, this reaction depends slightly on the sliding temperature and occurs the less prominent for 100°C and the most prominent for the 260°C sliding temperature.

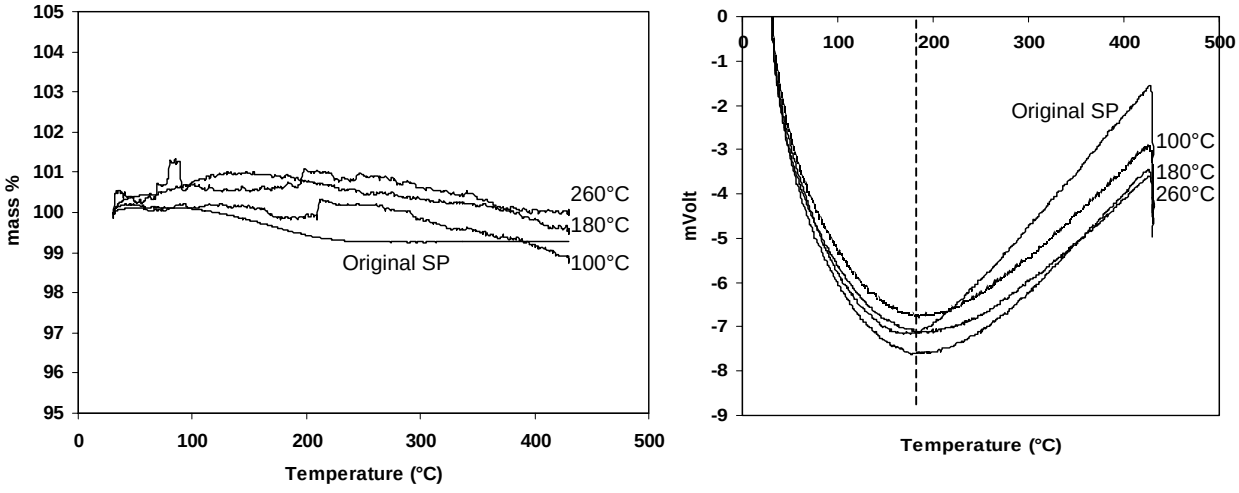

(a) (b)

Figure 5. Thermal analysis of polyimide wear debris for (a) TGA and (b) DTA measurements

3.3 Image processing techniques for characterisation of debris size and shape

The descriptions of wear morphologies as in paragraph 3.1 are frequently based on a qualitative description of the observed shapes and features. For obtaining however more quantitative information about its shape, mathematical analysis should be used for evaluation of the wear debris photographs. In this respect, the use of a Fourier spectrum and a morphological pattern spectrum will be illustrated, as these image processing techniques allow to extract parameters that relate to particle size and shape. Photographs of wear particles as obtained by optical microscopy look like the ones in Figure 3. The original pictures were colour images with resolution 1300 x 1030, but they are converted to 8 bit greyscale pictures since the applied image processing algorithms as presented below only work on monochrome images. For different sliding temperatures (100°C, 180°C) and normal loads (50 N, 100 N, 150 N), the wear debris images will be characterised by spectral analysis. Details about the calculation times for each of the spectra are given in ref. [8].

3.3.1 Fast Fourier Transform (FFT) spectrum of wear debris particles

The *Fourier transform* [9] of an original wear debris image results in an energy spectrum that is based on the greyscale periodicity in the image, representing a spatial frequency spectrum. Large image objects will have low frequency values and small objects will be represented by the higher frequencies. The Fourier transform lacks however the ability of spatial localisation, but in present case this is not a problem, since the debris particles don't have to be localised. The particles in the pictures don't behave periodically, but the size distribution should have its effect on the shape of the Fourier spectrum. A greyscale image as shown in Figure 3 is transformed with the two dimensional *Fast (Discrete) Fourier Transform* (FFT). This results in a two dimensional (real) spatial frequency energy spectrum (Figure 6a). In order to calculate some first-order histogram features and to remove the orientation dependence of the FFT-spectrum, the 2D-spectrum is transformed into a 1D-spectrum (FFTh) with on the abscissa the spatial frequency $\sqrt{(f_x^2 + f_y^2)}$ and for each of them an intensity (Figure 6b). The one dimensional FFTh spectra are calculated by Matlab™, allowing to compute the spectral Fourier parameters which are defined in Table 1, with b the histogram index and P(b) the histogram value divided by the image area. From the one-dimensional mean and maximum values plotted in Figures 6b and 7b, a variation in the debris spectra with increasing sliding temperature is already observed.

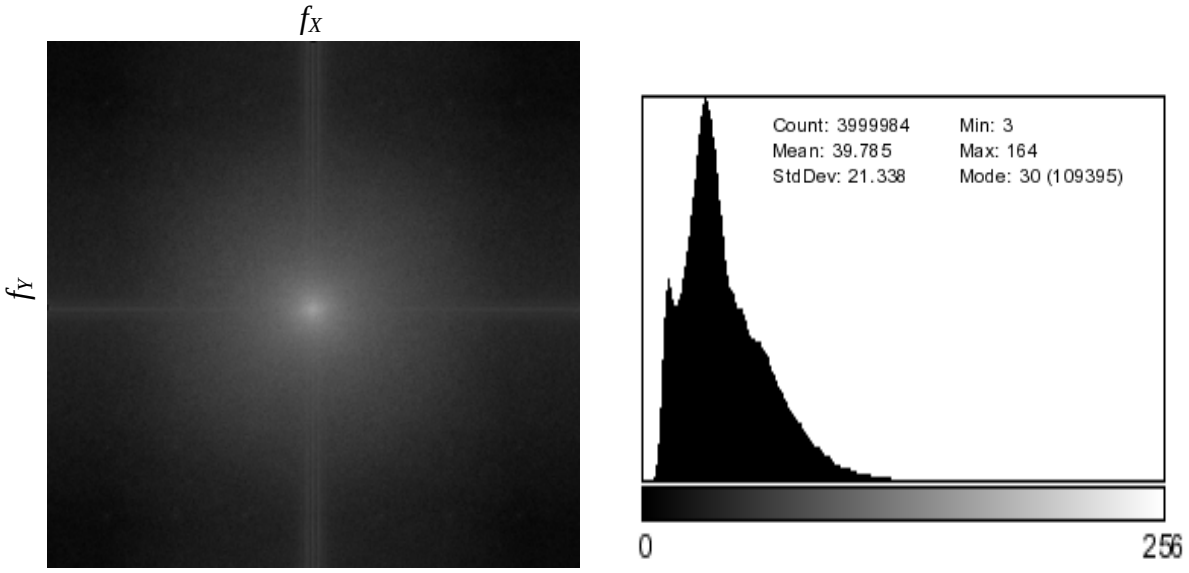

(a) (b)

Figure 6. Illustration of Fourier Transform of a greyscale wear debris image under 50N, 100°C, (a) two dimensional spectrum and (b) one dimensional spectrum

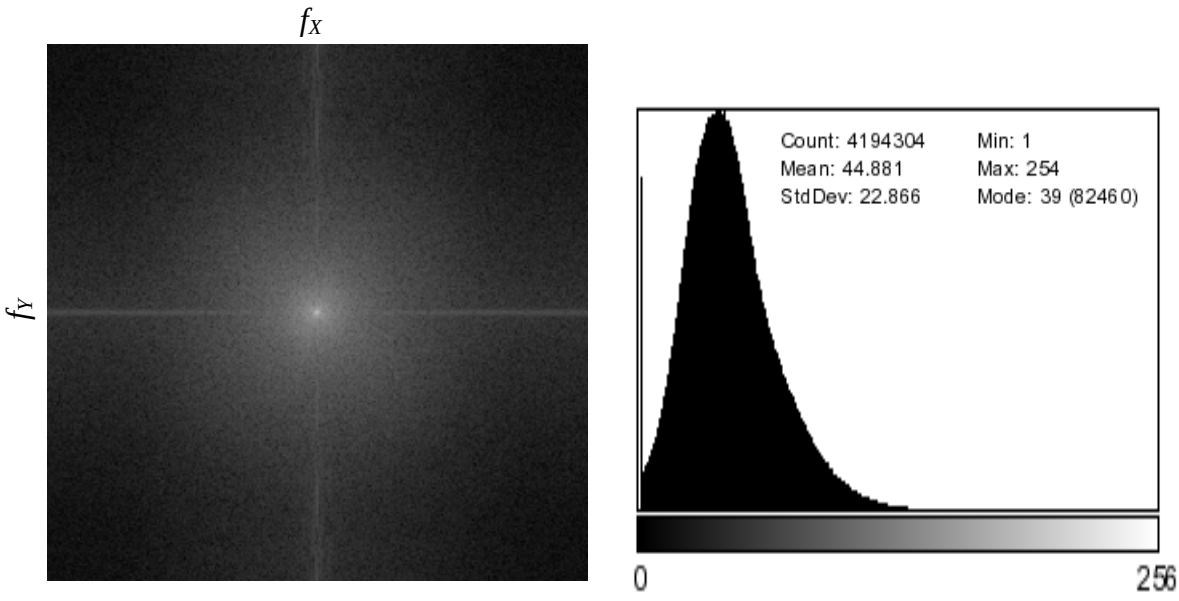

(a) (b)

Figure 7. Illustration of Fourier Transform of a greyscale wear debris image under 50N, 220°C, (a) two dimensional spectrum and (b) one dimensional spectrum

Mean	**Standard deviation**	**Skewness**
$S_M = \bar{b} = \sum_b bP(b)$	$S_D = \sigma_b = \left[\sum_b (b-\bar{b})^2 P(b)\right]^{1/2}$	$S_S = \frac{1}{\sigma_b^3}\sum_b (b-\bar{b})^3 P(b)$
Average histogram value	Spread of the histogram values	Asymmetry of the histogram curve
Kurtosis	**Energy**	**Entropy**
$S_K = \frac{1}{\sigma_b^4}\sum_b (b-\bar{b})^4 P(b) - 3$	$S_N = \sum_b P(b)^2$	$S_E = -\sum_b P(b)\log_2 P(b)$
Curve shape relative to a normal distribution		

Table 1. Spectral parameters computed from a Fourier Transform histogram

The spectra as shown in Figure 6 and Figure 7 were analysed for different sliding temperatures and normal loads and the evolution of the various spectral parameters for each of the applied temperatures or normal loads under sliding is given in Table 2. Linearity between the applied sliding parameters and the spectral parameters are investigated. A correlation coefficient P is therefore calculated, representing a linear (positive value) or an anti-linear (negative value) evolution of the spectral parameter with the applied experimental sliding parameter. The larger the value of P, the stronger the linear or anti-linear relationship and it is important that P is close to the unit value for having a strong correlation. Also a value P' is calculated representing the probability of getting a correlation as large as the observed value by random chance. A fully true correlation establishes when the P' value is close to zero. These probabilities are however only calculated for the normal load parameter, as the evolution of spectral parameters with temperature are (until present) only based on the analysis of two images. Also for evaluation of normal loads, the P' value is reasonably large as only few images were

available to perform full statistic analysis. Although, some trends already become clear and illustrate the effectiveness in spectral analysis of wear debris images.

Experimental parameters		Fast Fourier Transform spectral parameters					
		S_M	S_D	S_S	S_K	S_N	S_E
Temperature F_N = 50 N	P	1	1	1	1	1	-1
Temperature F_N = 100 N	P	1	1	-1	-1	-1	1
Temperature F_N = 150 N	P	1	1	1	1	-1	1
Normal load T = 100 °C	P P’	-0.14 0.86	0.62 0.38	0.87 0.14	0.86 0.14	-0.009 0.99	-0.67 0.33
Normal load T = 180°C	P P’	-0.83 0.38	-0.25 0.84	0.44 0.74	0.41 0.73	-0.94 0.23	-0.63 0.57

Table 2. Correlation coefficients for Fourier spectra of wear debris at different sliding temperatures and normal loads

Based on the correlation coefficients, it seems that *temperature* is proportional to the mean histogram value S_M, indicating that the particle size increases with higher sliding temperature. This calculated tendency is in good correspondence with the occurrence of agglomerated particles and the physical interpretation as given in paragraph 3.1. Also the spread in particle size increases proportionally with higher temperatures due to the occurrence of an important amount of large agglomerated particles besides the scale like wear debris at higher temperature. This agglomerated debris amount also explains the increase in spread under 50 N and 150 N with higher temperature, although other evolutions are calculated under 100 N normal load.

The *normal load* is inversely proportional to the mean histogram value, indicating that the particle size uniformly decreases when higher normal loads are applied under sliding, possibly due to fracture of the sintered structure. This trend becomes more probable when the sliding temperature is increased. For both 100°C and 180°C, and increase in normal load shows an identical decreasing relation in the spectral entropy (relation coefficient -0.63 to -0.67), with an average good probability P’.

3.3.2 Mathematical morphology (MM) spectrum of wear debris particles

Mathematical morphology (MM) [10] is based on the set theories, where morphological operations simplify image data, preserving the objects’ essential shape and size characteristics and eliminating irrelevant objects. A morphological filter element is used for scanning the image and depending on the size of the filter, objects are removed or maintained. The main advantage of a morphological filter for example is the ability to preserve the shape of large enough objects, unlike a Gaussian filter, which blurs small and big objects indiscriminately. The shape of the filter element can be determined in advance to include information about the image objects that should be analysed. If mostly circular objects are observed on the image, a circular filtering element should be chosen, while a rectangular filtering element can be chosen for examination of rectangular objects. Two basic image operations are defined: a *dilatation*, which fills holes and smoothens the contour lines of an object, and *erosion*, which removes small objects and disconnects objects connected by a small bridge. Those operations are used prior to image analysis to correct for imperfections in the image objects. Some of the wear debris particles may overlap with each other and would be regarded at one large particle. Therefore they should be first separated by erosion. On the other hand, some wear particles possibly do not form

a closed contour and should be filled by a dilatation for analysing it as one single particle. Such operations are defined in terms of a structuring element, i.e. a small window that scans the image and alters the pixels within the window frame as a function of its content. A dilatation of image A with structure element B blows up the object, erosion lets it shrink. Other operations, like the *opening* (an erosion followed by a dilation) and the *closing* (a dilation followed by an erosion), are combinations of the basic operations and are subsequently used for the creation of a spectrum.

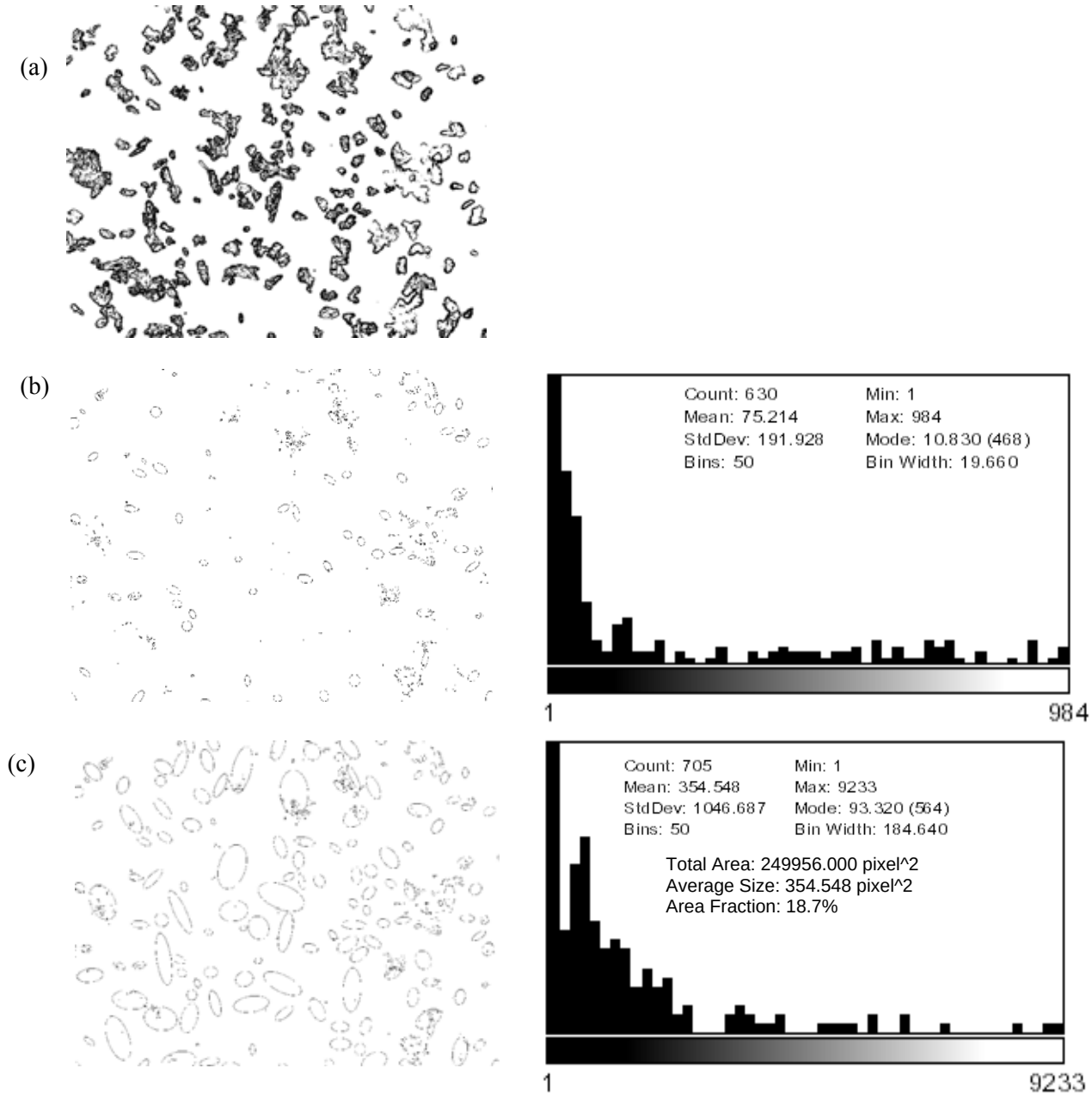

Figure 8. Mathematical opening operation performed on original greyscale image shown in (a), after increasing the size of the structural element from (b) 999 pixels to (c) 9999 pixels

If a structure element with given size and shape is given for performing an opening on an image, some elements will disappear. If the size of the structure element is increased, then more elements in the image will vanish. In this way it can be determined how the number of eliminated pixels increases when the image is morphologically opened using structure elements with progressive increasing sizes. The resulting plot of the number of eliminated pixels versus the size of the structure element is called the *pattern spectrum* (PS) or the *granulometric curve*. The pattern spectrum is a histogram of the

distribution of the sizes of various objects displayed in an image. An example of the subsequent removal of polymer wear debris particles and the corresponding pattern spectrum is illustrated in Figure 8. The structure element presently chosen has an elliptical form with progressively increasing diameter. From the original picture in Figure 3 under 50 N, 100°C a replica is made in Figure 8a, corrected by erosion and dilatation. The pictures in Figure 8b and Figure 8c show the elliptical zones where elements has been removed after increasing the pixel size from 999 pixels towards 9999 pixels. Finally, all the wear particles were removed from the image.

There is an analogy with the Fourier spectrum: the low frequencies in the Fourier spectrum relate to the global features of the image or the smooth objects, the high frequencies to the details or the fast greyscale variations. Similarly, big structuring elements in the pattern spectrum show the global features of the image or the large and smooth objects, while small sized structural elements also preserve the details or the small and rough objects. From the pattern spectrum of image A with structural elements B of increasing size n, different parameters as in Table 3 can be calculated.

Mean object size	**Entropy**
$S(A;B) = \frac{\sum_n nPS(A;B)(n)}{\sum_{a\in A} A(a)}$ Area	$E(A;B) = -\frac{\sum_n PS(A;B)(n)\log_2 \frac{PS(A;B)(n)}{\sum_{a\in A} A(a)}}{\sum_{a\in A} A(a)}$ quantification of the shape-size complexity
B-Shapiness	**N_{max}**
$BS(A;B) = \frac{PS(A;B)(N_{max})}{\sum_{a\in A} A(a)}$ quantification of the resemblance of the objects to the strel shape	The last bin (the highest *n*-value, when all image objects are sieved out) of the pattern spectrum histogram

Table 3. Characteristic parameters computed from a Pattern Spectrum

Experimental parameters		**Morphological Pattern spectral parameters**			
		S(A;B)	E(A;B)	BS(A;B)	N_{max}
Temperature F_N = 50 N	P	-1	1	-1	-1
Temperature F_N = 100 N	P	-1	-1	-1	-1
Temperature F_N = 150 N	P	-1	-1	1	-1
Normal load T = 100 °C	P P’	0.55 0.45	0.96 0.037	-0.79 0.21	0.88 0.12
Normal load T = 180°C	P P’	0.98 0.14	0.95 0.20	0.51 0.66	0.93 0.23

Table 4. Correlation coefficients for Morphological pattern spectra of wear debris at different sliding temperatures and normal loads

The spectrum was calculated for a structure element starting at size 2 x 2 pixels, increasing until all of the wear particles were resolved. The four parameters listed in Table 3 were calculated for each of the spectra and the correlation coefficients P together with probability factors P’ between the experimental sliding parameters and the spectral characteristics are given in Table 4. As however the calculation

time of the pattern spectrum on the entire image is too large, the original image was divided into 3 x 4, 10 x 10 and 20 x 20 subimages that were processed independently for calculation of the spectra and the different subimages were afterwards matched. The calculated spectra for the full image and the subimage divided original image are shown in Figure 9, where it is seen that mainly the N_{max} for the 3 x 4 - case is higher than the one for the original image. This is due to boundary effects. When the number of subimages increases, the values of size, N_{max} en entropy decrease. The values of shapiness increase. When the number of subimages is increased, the spectra show higher values, although this trend diminishes when the size of the structural element is larger.

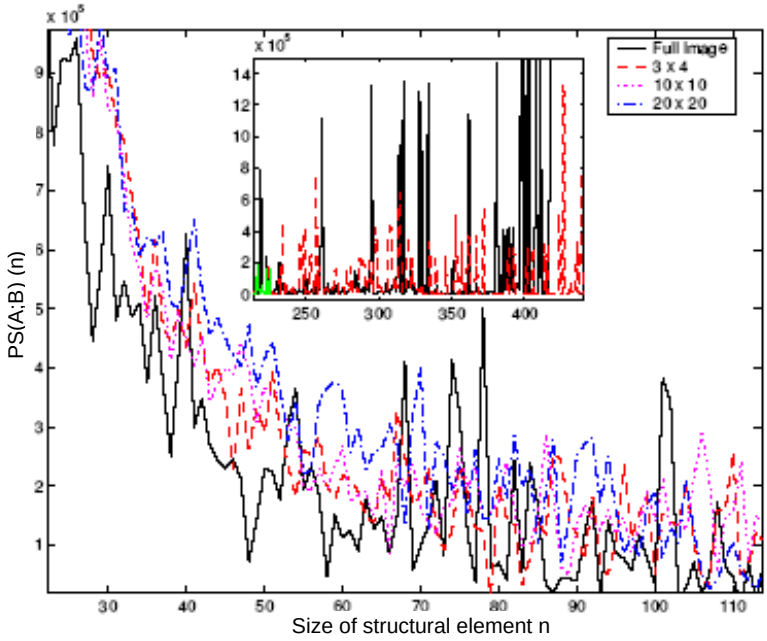

Figure 9. Pattern Spectrum of the original (full) image and the into subimages divided images.

Another technique for reducing the calculation time is the use of an Area Pattern Spectrum (APS), where also the shape of the wear debris particles is taken into account but however, instead of using a structural element, there is a threshold value defined which will now decide which components will be removed from the image. For generation of the area spectra, threshold values of 2, 4, 9, 16, 25, … were used. The correlation coefficients P and probability factors P' are calculated in Table 5.

Experimental parameters		**Area Pattern spectral parameters**			
		S(A;B)	E(A;B)	BS(A;B)	N_{max}
Temperature F_N = 50 N	P	1	1	1	1
Temperature F_N = 100 N	P	1	1	-1	1
Temperature F_N = 150 N	P	-1	-1	-1	-1
Normal load T = 100 °C	P P'	0.95 0.049	0.93 0.067	0.61 0.39	0.95 0.051
Normal load T = 180°C	P P'	0.016 0.99	0.13 0.92	-0.34 0.78	-0.001 0.99

Table 5. Correlation coefficients for Area pattern spectra of wear debris at different sliding temperatures and normal loads

Comparing both the Morphological pattern spectrum and the Area pattern spectrum shows that the processing parameters of and choice of structural element and/or threshold limit has important influence on the final spectral result. It should therefore be compared to the Fourier transform spectrum and a physical interpretation of the observed wear debris morphology.

Concerning the evolution of the spectral parameters with *temperature*, there is little correspondence between the morphological spectrum and the area pattern spectrum, where the mean particle size and N_{max} either increase or decrease with increasing temperatures. However, compared to the Fourier transform and the physical interpretation of agglomerated particles that are formed under higher sliding temperature, the area pattern spectrum (with proper selection of the threshold limit) provide the most reliable results indicating an increasing size and N_{max} value with temperature for 50 N and 100 N normal loads. The different trend in pattern spectra can be possibly related to the choice of the elliptical structure element and other geometries should be further examined. Regarding the effect of the *normal loads* under sliding, there is good agreement between the pattern spectrum and the area pattern spectrum, except for the B-shapiness. This observation confirms that another selection of shape for the structural element in the pattern spectrum should be made. Moreover, the area pattern spectrum seems more reliable due to the low values of the probability coefficients P' that should be close to zero for obtaining high probability. Parameters calculated from an area pattern spectrum, taking into account the wear debris shape and size generally provide better correlation with experimental sliding conditions, compared to the FFT parameters, taking into account a proper selection of threshold value that was presently determined by experimental fitting procedures.

4. CONCLUSIONS

A transition in friction and wear for sliding of polyimides corresponds with the occurrence of large agglomerated polymer wear debris, consisting of original polyimide grains that are compacted during the sintering process. The optical micrographs of the polymer debris were evaluated by Fourier analysis and Mathematical Morphology, in order to calculate the spectral parameters of the respective spectra. It seems that Fourier Analysis corresponds well to the physical observations of large particle sizes at high temperatures. For the Mathematical spectra, taking into account the particle shape, the results depend strongly on the selection of the filter element and a threshold value. However, it seems that with good selection of a threshold value, the area spectral parameters correspond well to the physical observations and the calculated linearity and probability are stronger than for a pure morphological pattern spectrum.

References

[1] M.G. Jacko, P.H.S. Tsang, S.K. Rhee, Wear debris compaction and friction film formation of polymer composites, Wear, 1989, Vol.133, 23-38

[2] M.Q. Zhang, Z.P. Lu, K. Friedrich, On the wear debris of Polyetheretherketone: fractal dimensions in relation to wear mechanisms, Trib. Int., 1997, Vol. 30, 87-102

[3] R.L. Fusaro, Evaluation of several polymer materials for use as solid lubricants is space, Trib. Trans., 1988, Vol. 31, 174-181

[4] U.S. Tewari, J. Bijwe, Tribological Behaviour of Polyimides, Polyimides: fundamentals and applications, Marcel Dekker Inc. (1996), 533-583

[5] P. Samyn, P. De Baets, J. Van Craenenbroeck, F. Verpoort, G. Schoukens, "Orientation of polyimide sliding surfaces studied by Raman spectroscopy", SPE ANTEC 2005, 1-4 May 2005, Boston (US)

[6] Dupont, Vespel parts and shapes, Design Handbook (2000)

[7] R.L. Fusaro, Effect of Atmosphere and Temperature on Wear, Friction and Transfer of polyimide films, ASLE Transactions, 1978, Vol 21, 125-133

[8] A. Ledda, J. Quintelier, P. Samyn, P. De Baets, W. Philips, "Quantitative Image Analysis with Mathematical Morphology", ProRISK 2003, Veldhoven (Netherlands)

[9] W.K. Pratt, Digital image processing, John Wiley & Sons, 3rd edition (2001)

[10] P. Maragos, Pattern spectrum and multiscale shape representation, IEEE Transactions on pattern analysis and machine intelligence, 1989, Vol. 11, 701-716